CHAPTER II

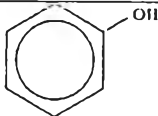# FUNDAMENTAL KNOWLEDGE AND LITERATURE REVIEW

2.1 Phenol

Phenol is the simplest aromatic alcohol which characterized by a hydroxyl (-OH) group attached to a benzene ring. The term phenol is not only for phenol itself but also for a class of aromatic compounds possessing a hydroxyl group attached to a benzene ring or a complex ring system. Phenol in water solution is sometimes called carbolic acid. Phenol differs from aliphatic alcohols which hydroxyl group is bonded to a saturated carbon atom. Due to the tendency of pi-orbital overlap between carbon and oxygen, phenol can lose easily the H^+ ion from the hydroxyl group, resulting in higher acidity than aliphatic alcohols (but weaker acidity than carboxylic acids). The intermediate state losing hydrogen ion (H^+) from the hydroxyl group in a phenol is called phenolate anion $C_6H_5O^-$. It reacts with strong bases to form salts called phenolates.

Pure phenol is a white crystalline solid. It is moderately soluble in water and is soluble in ethanol and ether. Phenols form stronger hydrogen bonds than aliphatic alcohols. Phenols are more soluble in water than alcohols and have higher boiling points. Many phenols have a sharp, spicy odour, but phenol smells bland and sweetish. It is highly toxic and caustic. Some phenols interfere with the endocrine system and disrupt the function of hormones. They have antiseptic property and are used in formulating disinfectants, deodorizers, and pesticides. Table 2.1 summarizes the important properties of phenol.

Phenol exists naturally and is manufactured in large quantity. It is found in nature in some foods, in human and animal wastes, and in decomposing organic material. It is produced by the body and excreted independent of external exposure or intake. It is used primarily as an intermediate in the production of phenolic resins. The main sources of phenolic wastewater are the industries such as petrochemicals, coal gasification, pesticide manufacture, and electroplating and metallurgical operations.

Many researchers studied the photocatalytic degradation of phenol by titanium dioxide nanoparticles that this process could decompose and mineralize the phenol solution effectively. The product of complete photocatalytic reaction was carbon dioxide and water. In addition, they found that the degradation products, such as catechol, hydroquinone, benzequinone, and pyrogallol could occur, if the photocatalytic reaction was not complete (Barni $et\ al.$, 1995). The dark adsorption of phenol on TiO_2 had been studied: Kusvuran $et\ al.$, (2005) found that the most adsorption of phenol on TiO_2 occurred within 15 min, Wang $et\ al.$, (2004) found that adsorption-desorption equilibrium of phenol on TiO_2 occurred for 60 min, while Valtierra $et\ al.$, (2004) found that equilibrium concentration of phenol on TiO_2 in dark adsorption was reached in less than 120 min.

Table 2.1 The important properties of phenol.

Molecular structure	
Molecular weight	94.1
Application	Additive component
Boiling point (^{0}C)	182
Melting point (^{0}C)	41
Specific gravity	1.07
Solubility in water (g cm^{-1})	0.08

2.2 Titanium dioxide photocatalyst

Photocatalyst can be defined as the catalyst involving light absorption that it provides the catalytic reaction. In the photocatalytic oxidation process, the semiconductor is used as the photocatalyst. The structure of semiconductor consists of two energy bands: conduction band and valence band. Conduction band is separated from valence band by band gap, which its width is equal to band gap energy (E_{bg}) of each semiconductor. The band gap energy of a semiconductor is the minimum energy of light required to make the material electrically conductive, or, in other words, to get the electrons excited enough to get moving (Oppenlander, 2002).

TiO_2 is one of the most widely used photocatalyst for heterogeneous photocatalysis due to its activity, photostability, non-toxicity, commercial availability, large band gap energy, etc. Its absorption spectrum overlaps with the solar spectrum and hence opens up the possibility of using solar energy as the source of irradiation. Another advantage is that the photocatalytic activity of TiO_2 can be studied in the

fixed bed form as well as in the form of a suspension (Devipriya *et al.*, 2005). The photocatalytic activity of it is depended on its crystallinity and particle size. In nature, it can exist in three crystalline phases (see Fig. 2.1): rutile (tetragonal, a=0.4593 nm, c=0.2959), which tends to be more stable at high temperature and thus is sometimes found in igneous rocks, anatase (tetragonal, a=0.3785 nm, c=0.9514), which tends to be more stable at lower temperature, and brookite (orthorhombic, a=0.5436 nm, b=0.9166, c=0.5135), which is usually found only in minerals (Park *et al.*, 2005). The TiO$_2$ of the anatase phase shows a higher photoactivity than the other phases of TiO$_2$ and having a band gap energy E_{bg} of 3.2 electron volts (eV), which corresponds to UV light of 388 nm (Fujishima *et al.*, 1999). Comparisons of the principle properties of the rutile and anatase types of TiO$_2$ are tabulated in Table 2.2.
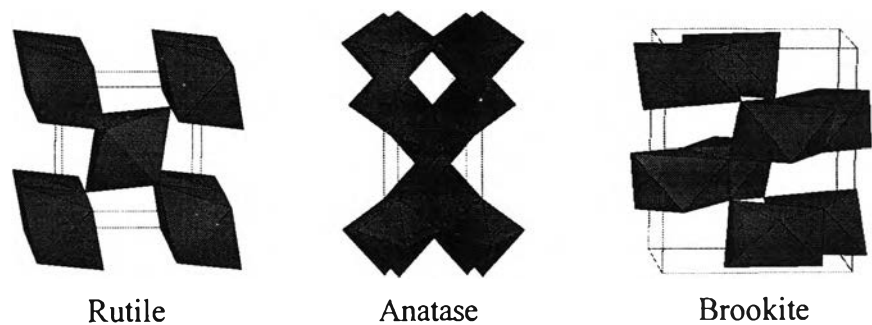

| Rutile | Anatase | Brookite |

Figure 2.1. Crystalline phase of TiO$_2$.

Table 2.2 Comparison of rutile and anatase. (Fujishima *et al.*, 1999)

Properties	Rutile	Anatase
Crystalline form	Tetragonal system	Tetragonal system
Specific gravity	4.2	3.9
Refractive index	2.71	2.52
Hardness	6.0-7.0	5.5-6.0
Permittivity	114	31
Melting point (^{0}C)	1858	Changes to rutile at high temperature

2.3 Photocatalytic reaction

Photocatalytic reaction is a process in which electrons in the catalyst could be accelerated from its ground to excited state, leading to stimulation of reactants to undergo reaction to form some products depending on the mechanism of photoreaction (Oppenlander, 2002). The advantages of the photocatalytic process are including (Devipriya *et al.*, 2005):

1) Complete oxidation of organic pollutants within few hours.

2) No formation of polycyclic products.

3) Availability of highly active and cheap catalysts capable of adapting to specially designed reactor system.

This process is upon with UV irradiation of a semiconductor. When a semiconductor (e.g. TiO_2) absorbs a photon with energy equal to or greater than its band gap energy, the formation of an electron/hole pair can be occurred. An electron is promoted from the valence band to the conduction band (e_{CB}^-) leading to occurring of hole in the valence band (h_{VB}^+). If charge separation is maintained, recombination is

prevented and subsequent redox reactions with absorbed substances may occur. At solid-liquid interface, e_{CB}^- can transfer from conduction band to electron acceptor in solution (reduction) and electron from donor in solution can capture with h_{VB}^+ in valence band (oxidation). The mechanism of photocatalytic reaction is shown in Fig. 2.2.
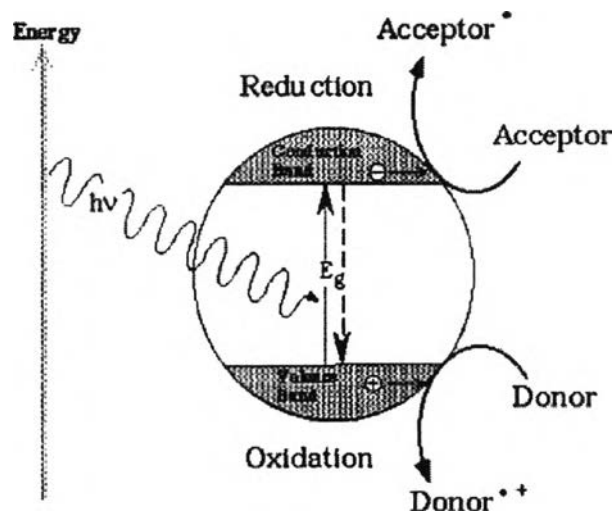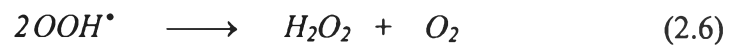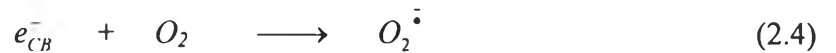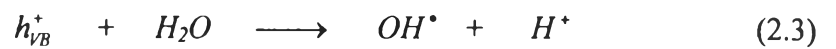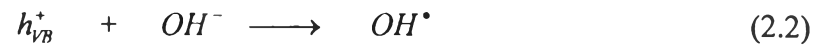

Figure 2.2. Principle mechanism of photocatalytic reaction. (Bahnemann, 2004)

Briefly, h_{VB}^+ reacts with H_2O or OH^- to generate the hydroxyl radical ($OH^\bullet$) at the surface and e_{CB}^- is reduced by molecule oxygen to generate the superoxide ion radical ($O_2^{\bullet-}$). The superoxide radical anion reacts subsequently with H^+ to produce perhydroxyl radical ($OOH^\bullet$) and following hydrogen peroxide (H_2O_2). Hydrogen peroxide can receive the energy from photon to produce the hydroxyl radical. The hydroxyl radical is the oxidizing specie in the photocatalytic reactor process, which it can decompose the organic pollutants that present at or near the surface of TiO_2 (Bahnemann, 2004). The photocatalytic reaction process with TiO_2 as a semiconductor can be represented in the following reactions;
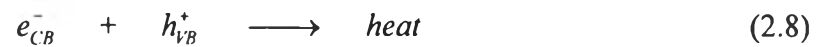
I) Excitation

$$TiO_2 \quad + \quad h\upsilon \quad \longrightarrow \quad e^-_{CB} \quad + \quad h^+_{VB} \qquad (2.1)$$
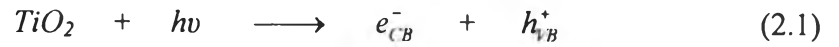
II) e-/h+ trapping and radical formation

$$h^+_{VB} \quad + \quad OH^- \quad \longrightarrow \quad OH^{\bullet} \qquad (2.2)$$

$$h^+_{VB} \quad + \quad H_2O \quad \longrightarrow \quad OH^{\bullet} \quad + \quad H^+ \qquad (2.3)$$

$$e^-_{CB} \quad + \quad O_2 \quad \longrightarrow \quad O_2^{\bullet -} \qquad (2.4)$$

$$H^+ \quad + \quad O_2^{\bullet -} \quad \longrightarrow \quad OOH^{\bullet} \qquad (2.5)$$

$$2OOH^{\bullet} \quad \longrightarrow \quad H_2O_2 \quad + \quad O_2 \qquad (2.6)$$

$$H_2O_2 \quad + \quad h\upsilon \quad \longrightarrow \quad 2OH^{\bullet} \qquad (2.7)$$

III) Recombination

$$e^-_{CB} \quad + \quad h^+_{VB} \quad \longrightarrow \quad heat \qquad (2.8)$$

The overall process can be summarized as follows:

$$organic\ pollutants \quad + \quad O_2 \quad \xrightarrow[semiconductor]{h\upsilon \geq E_{bg}} \quad mineralized\ products \qquad (2.9)$$
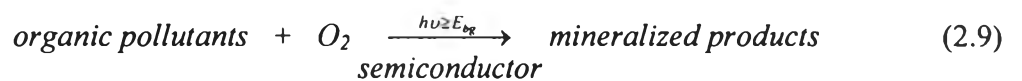
2.4 The pollutants removal using titanium dioxide

In the last decade, many studies have employed the titanium dioxide for solving the environmental problems. There are many techniques to treat or clean air and water as follows:

Suspend the titanium dioxide in wastewater: many reporter used this method to treat the impurity in water which was toxic and hardly biodegradable due to this method was acknowledged that easy to find the kinetic or rate of titanium dioxide.

Viriya-empikul, (2004) investigated the decomposition of organic compounds: methylene blue, Black 5, and lignin by using titania (code name: M1, M2, T1, T2, and N1) of different crystallite sizes. The selected titania (2 mg) was suspended in 20 cm^3 aqueous solution of each organic compound while shaking to ensure good dispersion of the titania in each sample. T1-titania decomposed Black 5 faster and better than M2-titania but M2-titania decomposed methylene blue faster than T1-titania. T1-titania was chosen to study in the titania cake layer system to avoid losing titania with the treated wastewater. This system, which cake thickness was 0.08 cm and this cake formed on HEPA filter, could prevent 99.9% titania loss at very low total removal efficiency of Black 5 (6%) and in contact time 0.88 min.

Qamar *et al.*, (2005) studied the effects of type of TiO_2 (Degussa P25, Hombikat UV100, PC500), reaction pH (3-9), catalyst concentration (0.5-5 g dm^{-3}), substrate concentration (0.25-0.75 mM), and electron acceptors (H_2O_2, $KBrO_3$, $(NH_4)_2S_2O_8$) on the photodegradation and photomineralization process of chromotrope 2B and amido black 10B. The results showed that the degradation rate and mineralization rate were strongly influenced by all the above parameters. Degassa P25 showed superior photocatalytic activity as compared with the other

photocatalysts. The chromotrope 2B was degraded faster than the amido black 10B. The photodegradation efficiency and photomineralization efficiency of both dyes increased with increasing reaction pH. All electron acceptors showed the beneficial effect for the degradation and mineralization of chromotrope 2B, while amido black 10B was enhanced the degradation and mineralization by only $KBrO_3$.

Kusvuran *et al.*, (2005) evaluated the photocatalytic degradation of different substituted and isomers of phenols, namely, 2,4,6-trimethylphenol (TMP), 2,4,6-trichlorophenol (TCP), 2,4,6-tribromophenol (TBP), 2,4-dimethylphenol (DMP), 2,4-dichlorophenol (DCP) and 2,4-dibromophenol (DBP) by TiO_2/UV. They found that TCP showed the fastest degradation and TMP showed the slowest degradation. Degradation rate constants have been observed to be extremely depended on electronegativity of the substituents on phenolic ring. Photocatalytic degradation kinetics of all phenolic compounds had been explained in terms of Langmuir–Hinshelwood kinetics model. Degradation rate constant and adsorption equilibrium constant of TCP were calculated as k 0.0083 mM min^{-1} and K 9.03 mM^{-1}. For TBP and TMP the values of k and K were obtained as 0.0040 mM min^{-1}, 19.20 mM^{-1}, and 0.0017 mM min^{-1}, 51.68 mM^{-1}, respectively. Degradation rate constant of DBP was similar as DCP (0.0029 mM min^{-1} for DBP and 0.0031 mM min^{-1} for DCP) whereas adsorption equilibrium constants differed (48.40 mM^{-1} for DBP and 30.52 mM^{-1} for DCP). K and k of DMP found as 83.68 mM^{-1} and 0.0019 mM min^{-1}, respectively. The adsorption equilibrium constants in the dark were ranged between 1.11 and 3.28 mM^{-1} which are lower than those obtained in kinetics.

Irmak *et al.*, (2004) studied the degradation of 4-chloro-2-methylphenol (PCOC) in aqueous solution by UV irradiation in the presence of TiO_2. They found that only 51.4% of PCOC was degraded. They then improved the efficiency of

degradation process by adding oxidants as electron scavenger in this solution. Periodate ion was found to be much more efficient oxidant than the others in improving the degradation of PCOC via formation of reactive species. The effect of the oxidants used in the UV/TiO_2 systems on the degradation rate of PCOC were found to be in the order of $IO_4^- > BrO_3^- > H_2O_2 > O_2 > ClO_3^-$. In addition, addition of metal ions to $UV/TiO_2/H_2O_2$ system increased the degradation rate of the organic substrate. The effect of Mn^{2+}, Cr^{3+}, Fe^{2+} and Fe^{3+} metal ions on degradation of PCOC in the $TiO_2/UV/H_2O_2/M^{n+}$ system was found to be in the order of $Fe^{3+} > Fe^{2+} > Mn^{2+} > Cr^{3+}$. The adsorption equilibrium constant and the rate constant were determined to be 74.16 mM^{-1} and $0.0081 \text{mM min}^{-1}$, respectively.

Swarnalatha *et al.*, (2004) studied on the heterogeneous photocatalytic oxidation of 2,6-dinitrophenol with different catalysts like TiO_2, TiO_2-P25, CdS, WO_3, and ZnO using an annular-flow type photo reactor with a 8W low pressure mercury lamp as a UV light source. They found that TiO_2-P25 was the most efficient as photocatalyst when compared to other catalysts due to its photo stability. The degradation was about 88.1% and occurred by irradiation for 240 min and the maximum degradation was observed at the catalyst concentration of 4 g dm^{-3}. In the case of oxygenated system, the complete photodegradation could be attributed within 3.5 h of the irradiation period. For the same time interval in the case of nitrogenated system, 73% of photodegradation was observed.

Supported on substrate, and used as thin film: many attempts had to solve the problem of the titanium dioxide loss during filtration and elutriation by various applications such as synthesized composite material which high efficiency and easily recovery, and used as thin film.

Zhang *et al.*, (2000) proposed the rotating-drum reactor coated with a TiO_2 photocatalyst in which Pt-loaded TiO_2 powder was immobilized on the outer surface of a glass-drum for degrading phenol. The amount of Pt-loaded TiO_2 per unit area of glass drum was 11.4 g m^{-2}. This reactor showed that phenol could be decomposed rapidly under solar light since it could receive solar light and oxygen from the atmosphere effectively. Phenol with initial concentration of 22.0 mg dm^{-3} was degraded within 60 min and was completely mineralized to CO_2 and intermediate products within 100 min. The photonic efficiency under solar light was 0.00742 mol-C/Einstein. In the experimental, the influence of aeration and the rotation speed on the degradation process was studied. They found that the degrading phenol between when aerated and not aerated was not different, which it showed that the advantage of this reactor in saving energy. The optimal rotation speed was 25 rpm.

Bhattacharyya *et al.*, (2004) investigated the performance of TiO_2 supported on three kinds of adsorbents: mesoporous (MCM-41), microporous (β-zeolite), and pillared structure (montmorillonite) where different loading (10-80%) of TiO_2 was prepared by sol-gel method and compared the synthesized catalysts with the bare TiO_2 produced by sol-gel method and commercial catalyst, Degussa-P25 in degrading an azo-dye, orange II. These supported catalysts were characterized by several analytical techniques including XRD, SEM-EDX, XPS, and BET analyzer. All supported catalysts exhibited good photodegradation efficiency of orange II and their overall removal efficiency was better than the bare TiO_2 produced by sol-gel method and commercial catalyst, Degussa-P25. TiO_2-MCM-41 and TiO_2-β-zeolite were better degrading orange II than TiO_2-montmorillonite, while the adsorption of orange II was maximum on TiO_2-montmorillonite.

Grzechulska *et al.*, (2003) investigated the photocatalytic oxidation of phenol in the labyrinth flow reactor with immobilized Degussa P25 photocatalyst. They observed that the photocatalytic material losses its activity during repeated test trials for the high initial phenol concentration of 300 mg dm^{-3} due to the diffuse reflectance UV-Vis analysis showed shift in the threshold absorption value and corresponding band gap energy of the photocatalytic material and FTIR analysis revealed the carbon deposits on the catalyst surface.

Nonami *et al.*, (2004) developed the apatite-coated TiO$_2$ photocatalyst by soaking the TiO$_2$ powder in a PBS (pseudo-body solution) containing an excess of phosphate ions at 37 ^{0}C for 1 h. The weight ratio of apatite to TiO$_2$ in synthesized photocatalyst found that 6 wt.%. This photocatalyst could absorb and decompose bacteria and other materials effectively which, the apatite phase can adsorb substances even without exposure to light and this substances can be decomposed by TiO$_2$ when exposure to light.

Fabiyi *et al.*, (1999) synthesized the TiO$_2$ coated onto naturally buoyant polystyrene beads using a thermal treatment procedure for investigating the photocatalysed mineralisation of methylene blue. The coated beads showed high mechanical stability as well as impressive photocatalytic activity. Thermogravimetric analysis of the beads, post-treatment, indicated that there was no destructive degradation of the polystyrene support by the photocatalytic degradation process. The catalyst activity remained appreciably high for up to 10 successive runs. For the buoyant particles, suspension was only possible for situations where pulsatile mixing was applied. Reaction rates in this system were found to increase with increase both in the catalyst loading and the pulsing conditions.

2.5 Filtration fundamental

Filtration, in which the solid-liquid mixture is directed towards a medium (screen, paper, membrane, etc.) involves with liquid phase or filtrate flows through the solids are retained on the surface of medium. The surface deposition mode depicts in Fig.2.3 is described by two serial resistances to fluid flow:

1) The resistance of the filter medium
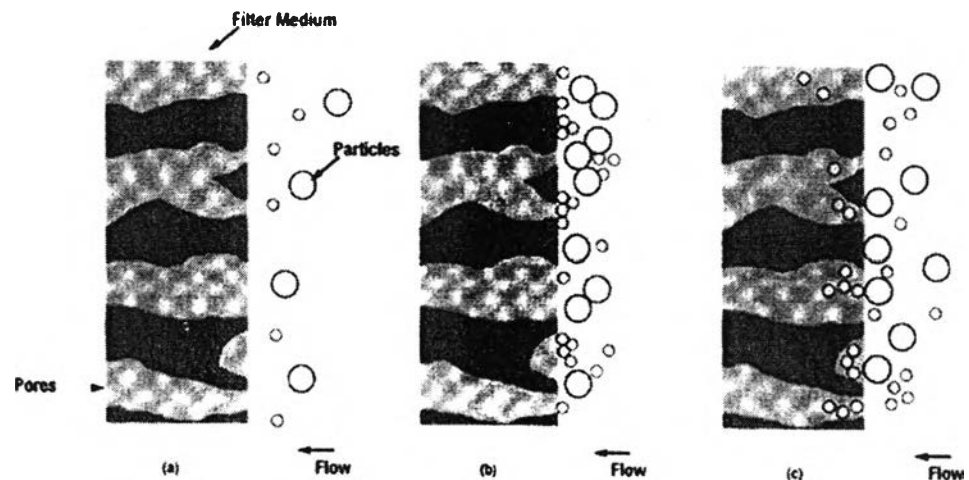
2) The resistance of the particulate layer or cake

Figure 2.3. Particle deposition in filtration. (Rushton *et al.*, 2000)

The relation between the pressure drop and the filtration rate of liquid passing through a packed bed of solids is divided into two types:

1) constant pressure filtration

2) constant rate filtration

In case of the experiment, the relation between the pressure drop and the filtration rate is a constant pressure filtration, thus:

$$\frac{t}{V} = \frac{\mu c \alpha}{2A^2 \Delta P} V + \frac{\mu R_m}{A \Delta P} \qquad (2.10)$$

For incompressible cake, terms of c and R_m are constant. Equation (10) is a straight line, whereas t/V is the dependent variable and V is the independent variable so, a graph of experimental data points of t/V against V permits the calculation of the gradient and intercept of this equation, which the gradient and intercept are as follows:

$$Gradient = \frac{\mu c \alpha}{2A^2 \Delta P} \qquad (2.11)$$

$$Intercept = \frac{\mu R_m}{A \Delta P} \qquad (2.12)$$

The liquid passes through the open space between the particles that is the pores or voids within bed. As it flows over the surface of the solid packing frictional losses lead to a pressure drop. The amount of solids inside the bed is important, namely, the greater this is the larger will be the surface over which liquid flows, therefore the higher the pressure drop will be occurred.